

Characterization and 3D printability of poly (lactic acid)/acetylated tannin

Jingjing Liao, Nicolas Brosse, Antonio Pizzi, Sandrine Hoppe, Xiaojian Zhou, Guanben Du

▶ **To cite this version:**

Jingjing Liao, Nicolas Brosse, Antonio Pizzi, Sandrine Hoppe, Xiaojian Zhou, et al.. Characterization and 3D printability of poly (lactic acid)/acetylated tannin. Industrial Crops and Products, 2020, 149, pp.112320. 10.1016/j.indcrop.2020.112320 . hal-02508080

HAL Id: hal-02508080

https://hal.univ-lorraine.fr/hal-02508080

Submitted on 13 Mar 2020

HAL is a multi-disciplinary open access archive for the deposit and dissemination of scientific research documents, whether they are published or not. The documents may come from teaching and research institutions in France or abroad, or from public or private research centers.

L'archive ouverte pluridisciplinaire **HAL**, est destinée au dépôt et à la diffusion de documents scientifiques de niveau recherche, publiés ou non, émanant des établissements d'enseignement et de recherche français ou étrangers, des laboratoires publics ou privés.

Characterization and 3D printability of poly (lactic acid)/acetylated tannin composites

Jingjing LIAO[a,b,c], Nicolas BROSSE[b]*, Antonio PIZZI[b], Sandrine HOPPE[c], Xiaojian ZHOU[a]*, and Guanben DU[a]

[a] Key Laboratory for Forest Resources Conservation and Utilisation in the Southwest Mountains of China (Southwest Forestry University), Ministry of Education, Kunming, 650224, PR China
[b] LERMAB, University of Lorraine, Boulevard des Aiguillettes BP 70239,54506 Vandœuvre-lès-Nancy, France
[c] LRGP, University of Lorraine, 1, Rue Grandville, BP 451, 54001 Nancy Cedex, France
* Correspondence: nicolas.brosse@univ-lorraine.fr; xiaojianzhou@hotmail.com

Abstract: In this study, a three-dimensional (3D) printing filament prepared from poly (lactic acid) (PLA) and acetylated tannin via a twin-screw extruder was reported. The impact of acetylated tannin loading content on the final properties of the resulting composite materials and their 3D printability were investigated. The experimental results indicate that PLA can be compounded with up to 20 wt% acetylated tannin without any obvious deterioration in the tensile property. The resulting composites acquired better degradation rate in aquatic system compared with neat PLA, especially in alkaline medium. Moreover, all composites are printable and showed generally good printing quality with brown color, however, this is limited to temperatures reasonably below 220°C to avoid printing defects, especially at high loadings of acetylated tannin.

Keywords: poly (lactic acid), acetylated tannin, composite, degradation, 3D printability

1. Introduction

Additive manufacturing, commonly known as three-dimensional (3D) printing, is a promising manufacturing technology whose related numerous applications have been explored in the fields like construction, manufacturing, healthcare and medicine, art and fashion, food industry (Lee et al., 2017; Liu et al., 2019). With this technique, customized complex and high-resolution three-dimensional parts can be rapidly built through

successive layer-by-layer deposition of materials like plastic, metal, ceramics, or living cells (Tappa and Jammalamadaka, 2018). For producing thermoplastics prototype parts, fused deposition modeling (FDM) or melt-extrusion 3D printing is the most widely used additive manufacturing technique.

Polylactic acid (PLA) is one of the most popular 3D printing thermoplastic materials due to its printability, favorable mechanical properties, and biocompatibility. It is an renewable and biodegradable polyester that can be synthesized directly through polycondensation of lactic acids or ring-opening polymerization of lactides (Ren, 2011). PLA can be also incorporated with sustainable materials or biopolymers (e.g. wood powder, plant fiber, cellulose, lignin, hemicellulose) for the purpose of reinforcing and/or specific functions, and/or reducing cost. However, studies of these PLA-based bio-composites as 3D printing materials are still limited (Bajpai et al., 2014; Basu et al., 2017; Murariu and Dubois, 2016). Sustainable materials or biopolymers applied as 3D printing feedstock are promising substitutes for fossil-based fillers due to their sustainability, biodegradability, and cost-efficient characteristics. For instance, the presence of wood powder in 3D printing, PLA filaments displays higher stiffness and less abrasive properties compared to other composite filaments, such as carbon-fiber filled PLA filaments and metal-filled PLA filaments (Guo et al., 2018). Fibers derived from wood, bamboo, and cellulose were also investigated as feedstock for PLA-based filaments because of their positive effects on the mechanical properties and heat resistance of PLA matrix (LI et al., 2016; Long et al., 2019). Hemicellulose has been investigated to partially replace PLA as feedstock material in 3D printing (Xu et al., 2018). This combination makes use of the characteristics of hemicelluloses such as biocompatibility, biodegradability, and presence of versatile active sites for biomedical applications. PLA combined with lignin has attracting characteristics such as antioxidant, antifungal and antimicrobial capacities, resistance to UV-radiation, and fire-retardant properties (Kai et al., 2016). One example was reported to study PLA/lignin composites for 3D printing (Gkartzou et al., 2017). However, the lignin aggregation and its low compatibility with PLA matrix caused imperfect printed objects and surface roughness,

even at low loading content (5 wt%.). According to the published literature as yet, it appears that the dispersion and distribution of fillers are key factors for processing 3D printing materials (Nguyen et al., 2018).

Condensed tannins are interesting abundant and sustainable biopolymers for 3D printing, however, there is no related research work about their applications in the field of 3D printing to date. Condensed tannins are mainly composed of flavonoid units in varying degrees of condensation (**Erreur ! Source du renvoi introuvable.**) and they can be easily extracted from soft tissues of woody plants like leaves, needles, and bark using water or organic solvent (Pizzi, 1980). They display great potential as component of PLA bio-composites due to some interesting characteristics like antioxidant (Koleckar et al., 2008), antimicrobial (Ge et al., 2003) and stabilizing properties (Liao et al., 2019; Olejar et al., 2016; Tomak et al., 2018). Over the past few years, tannins have been investigated as functional additives or at least a component of polymeric composites. For instance, tannins have been reported as stabilizing additive with antioxidant and UV-protective properties on polypropylene (Ambrogi et al., 2011; Samper et al., 2013), polyethylene (Bridson et al., 2015), poly(vinylchloride) (PVC) (Shnawa et al., 2015), and polyvinyl alcohol (Zhai et al., 2018). Anwer reported a native tannin as a filling component of PLA composite material (Anwer et al., 2015), where poor adhesion between tannin and PLA matrix as well as dispersion of tannin in PLA were found, thereby, poor tensile strength was noticed even at higher filler content (15%). Modifications of tannins, like esterification and hydroxypropylation, have been proved to enhance the compatibility and dispersion capacity to various plastics (D. E. García et al., 2015; Gaugler et al., 2007; Grigsby et al., 2014, 2015, 2013; Grigsby and Kadla, 2014). Grigsby and co-workers (Grigsby et al., 2015) modified tannin with ester-bearing long chain, which lowered the melting temperature and claimed this could significantly reduce the incompatibility with PLA matrix, leading meanwhile to easier processability. However, the substitution of higher chain length on tannin flavonoid units becomes progressively more difficult due to the elevated steric hindrance. In another extended study, Grigsby carried out a high loading content of esterified tannin (50%) as

reinforcing material for PLA fine fiber processed via melt spinning in the presence of transesterification catalyst (Grigsby and Kadla, 2014). This successful incorporation of esterified tannin onto PLA indicated the possibility to process esterified tannin filled PLA filaments for 3D printing. Esterification can reduce the hydrophilicity of tannin, reducing the clogging at the printing nozzle and discontinuous layer deposition during printing process due to good dispersion and distribution of tannin onto the polymer matrix.

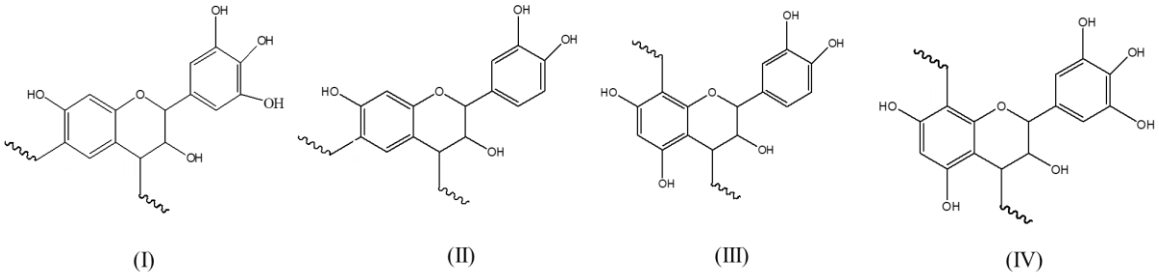


Figure 1. Structure of four main flavonoid units of condensed tannins

The present study will focus on developing a new approach to utilize condensed tannin obtained from mimosa wood barks for partial replacement of PLA in 3D printing parts and investigate the feasibility of melt-extrusion 3D printing. For this purpose, mimosa tannin was acetylated to decrease its initial hydrophilicity. Such treatment has been proven to enhance the compatibility of tannin and thermoplastic polymeric matrixes without severe agglomeration (Gaugler et al., 2007; Grigsby et al., 2013). The composite was processed in a twin-screw extruder and the impact of the loading level of acetylated tannin (AT) on the final properties of the resulting composite materials was evaluated in terms of the tensile property, the changes in crystallization, thermal degradation, changes in color, and degradation rate in aquatic system. Besides, the feasibility of melt-extrusion 3D printing of PLA/AT composite was also investigated.

2. Materials and Methods

2.1. Materials

PLA trademarked under the name IngeoTM Biopolymer (Grade 3D850) with a melt flow index of 7-9 g/10min was obtained from Nature works LLC (Minnesota, USA). Mimosa tannins were purchased from Silva Chimica, Mondovi, Italy. Acetic anhydride

used to acetylate tannin and pyridine, a catalyst for tannin acetylation, were supplied from Sigma-Aldrich and Acros-Organics, respectively. Three buffers purchased from Sigma-Aldrich were used for degradation tests, including phosphate buffer (pH=4.0), sodium carbonate buffer (pH=10.0), and phosphate Buffered Saline (PBS, pH=7.4).

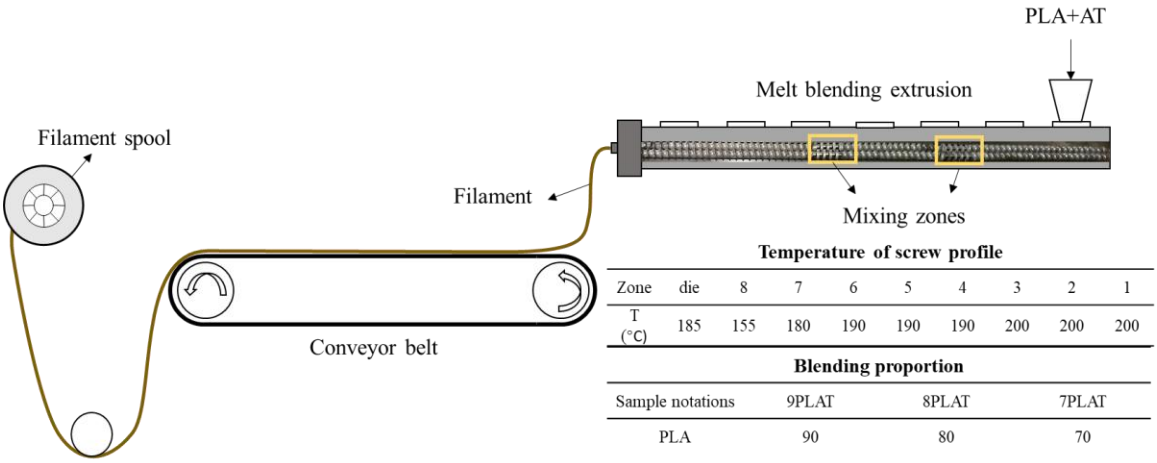
2.2. Preparation of PLA/AT Composites

2.2.1. Tannin acetylation

Acetylation of mimosa tannin was described elsewhere by using acetic anhydride and pyridine as catalyst (Nicollin et al., 2013). Mimosa tannin was mixed with acetic anhydride in a weight ratio of 1:5 with 1 wt% pyridine (based on tannin) as catalyst in a round bottom flask fitted with a condenser. The mixture was heated to 60°C under stirring for 6 h. After the acetylation is achieved, the suspension was precipitated in iced water and centrifuged to recover the acetylated tannin powder, which was washed 5 times with distilled water and finally air-dried at room temperature for several days.

2.2.2. Composite filament preparation

PLA was ground into powder by a grinder to ensure simplistic mixing with tannin. Then, PLA and acetylated tannin (AT) powder were dried in an oven at 80°C for more than 12 h to remove any absorbed water on the surface. A twin-screw extruder (Thermo Scientific^{TM} Process 11, Villebon-Sur-Yvette, France) was used to blend PLA powder and AT. Two mixing zones of screw profile can guarantee high level of homogeneous dispersion of AT in PLA. The temperature of the heating zones and the die along the extruder barrel ranged are shown in Figure 2. The filaments were extruded through melt blending extrusion with a rotation rate of 80 rpm via a nozzle diameter of 4 mm. A filament with a diameter of 1.75 ± 0.1 mm was obtained by controlling the speed of spool rotation and conveyer belts then the 3D printable filaments were collected by a spool.



Temperature of screw profile

Zone	die	8	7	6	5	4	3	2	1
T (°C)	185	155	180	190	190	190	200	200	200

Blending proportion

Sample notations	9PLAT	8PLAT	7PLAT
PLA	90	80	70
AT	10	20	30

Figure 2. Composite filaments preparation via melt blending extrusion: the tables show the parameters of screw profile and blending components proportions

2.2.3. 3D printing process

An open-source 3D printer named Mondrian 3.0 was used to print scaffold (20.1 × 20.1 × 3 mm) and standard dog bones (ISO 527, type 1A) using PLA/AT filaments at 190°C. Abundant of filament was needed to construct dog bone specimen, thus, we prepared only one dog bone specimen due to the limited filament amounts. The scaffolds were printed using PLA and PLA/AT composite filaments under three printing temperature (180°C, 200°C, 220°C). The used printing parameters are shown in Table 1. The scaffold and dog bone were designed by using a Slic3r program and printing process were controlled by Pronterface software.

Table 1. 3D printing parameters

Printing temperature	180 - 220°C
Layer height	0.2 mm
Infill density	100%
Infill pattern	linear
Layer angle	45°
Printing speed	12 mm/s

Nozzle diameter	0.4 mm

2.3. Characterizations

The acetylation of tannin was confirmed by NICOLET 6700 FT-IR spectrometer in attenuated total reflection (ATR) mode with a resolution of 4 cm^{-1} and a total of 16 scans in the range 400-4000 cm^{-1}.

Instron tensile testing machine (model 5569, Norwood, MA, USA) equipped with a 50 kN load cell was used for tensile strength tests with a cross-head speed 1 mm/min according to EN ISO 527:1996. The whole testing process was performed at room temperature and each sample has four repetitions. The tested dog-bone shaped specimens (ISO 527, type 1A) were previously molded with a micro-injection molder (Micro 15, DSM Xplore, Sittard, Netherlands).

A scanning electron microscopy (SEM, JSM-6490LV, Tokyo, JAPAN) with an acceleration voltage of 5 kV was applied to observe the morphology of a 3D printed scaffold. The scaffolds were sputter-coated with a thin layer of carbon before scanning.

A study on the thermal characteristics, in terms of the melting temperature (T_m) and crystallization temperature (T_c), was undertaken under a nitrogen flow of 50 mL/min by using a METTLER TOLEDO differential scanning calorimeter (DSC). A scanning rate of 10°C/min within the temperature range of 30°C to 220 °C and 220°C to -10°C in the second scanning cycle was carried out. The measurements were conducted using aluminum crucibles with a total sample weight of 5.00 ± 1 mg. The values for melting temperatures (T_m), enthalpies of melting (ΔH_m) and crystallization (ΔH_c) were analyzed using STARe software. ΔH_m^0 is the enthalpy of melting for 100% crystallized PLA, which is equal to 93.7 J/g (Yamoum et al., 2017), and w is the weight fraction of PLA. The crystallization percentage (X_c, %) was estimated using the following equation:

$$X_c\,(\%) = \frac{\Delta H_m - \Delta H_c}{\Delta H_m^0 \times w} \times 100\% \qquad (1)$$

The degradation behavior of AT-filled PLA was characterized with the help of a thermogravimetric analyzer (TGA, METTLER TOLEDO, Columbus, Ohio, USA) under air

flow of 50 mL/min from 30 to 600°C. The heating rate was controlled at 10°C/min and the weight of each sample was 5-10 mg.

Color measurements. PLA is a colorless and transparent polymer, thus, it generally colorize with dyes (Hussain et al., 2015; Scheyer and Chiweshe, 2001). Tannin can colorize PLA filaments due to its brown nature, which is a good feature for 3D printed parts. The coloration of PLA filaments with acetylated tannin was investigated by a spectrophotometer (X·rite, model 5P60, Regensdorf, Switzerland) based on the international commission on illumination (CIE) system. Three parameters L*, a* and b* were used to evaluate the colors of filaments, respectively. L* represents the scale of lightness, the value of 0-100 refers to perfect black to white. The value of a* and b* stands for the color of the red-green and the yellow-blue character, respectively, in which positive values represent redness or yellowness while negative values indicate greenness and blueness (Lai So et al., 2014).

Water absorption. The hydrophobicity of the filaments was characterized by measuring their level of water absorption (Filgueira et al., 2017). Each filament was cut into a length of 70 ± 1 mm and submerged into 50 mL of distilled water in a plastic tube for 30 days at room temperature. Before submerging the tested filaments into the water, the filaments were vacuum-dried for 6 h at 80°C and then measured the dried weight (W_0). After 30 days, the specimens were taken out from water and wiped using filter paper. Then the weight was recorded as W_1. The water uptake of PLA filaments and AT-filled filaments was calculated according to the following equation:

$$\text{Water absorption (\%)} = \frac{|W_1 - W_0|}{W_0} \times 100 \qquad (2)$$

Immersion in solvent. In order to understand the degradation of PLA/AT composites in aquatic system, printed specimens of dimensions 2.5 × 30 × 2 mm were immersed in buffer solutions (pH=4, pH=10) and PBS solution (pH 7.4) at 40°C for 50 days in an oven. The initial weight (W_0) of each specimen was recorded before soaking into the solvent in glass tube containing 50 mL buffer solution. After 50 days, the samples were removed from the tubes and washed 3 times with distilled water prior to final dry in oven at 40 °C

for 12 h. The weight of each specimen was denoted as W_1. The weight loss was calculated based on the equation (2).

3. Results and discussion

3.1. Characterization of acetylated tannin

The hydrophilic characteristic of tannin render it incompatible with hydrophobic or semi-hydrophobic polymers. This necessitates the modification of tannin for solving this problem. Tannin acetylation was suggested to develop reasonable miscibility with PLA (Grigsby and Kadla, 2014). Figure 3 presents the FTIR spectra of tannin and tannin after being acetylated. The spectrum of tannin reveals a broad band centered at 3250 cm^{-1} and can be ascribed to -OH stretching vibrations while the peak at 1614 cm^{-1} refers to aromatic ring stretching vibration. This latter signal corresponding to a function unaffected by the acetylation reaction which can be considered as an invariant band. Compared to the band at 1614 cm^{-1}, the sharp decrease of the -OH and emergence of a new strong one at 1750 cm^{-1}, which is typical of C=O stretching, representing ester functional group, proves that the acetylation process was undertaken effectively (Luo et al., 2010). Besides, the increased absorption at 1178 cm^{-1} and 1044 cm^{-1}, ascribed to C-O stretching, is also in accordance with the structure of acetylated tannin (Smith, 2018; Vila et al., 2016).

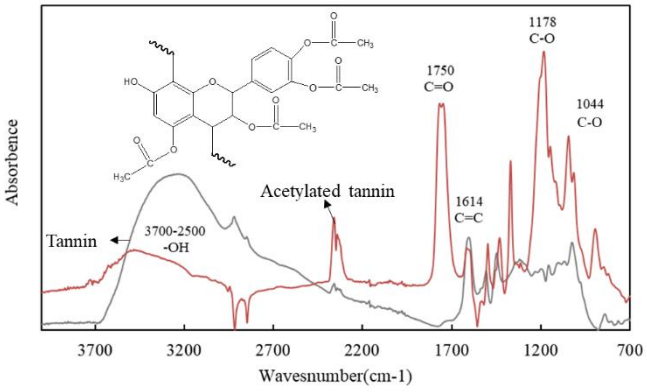
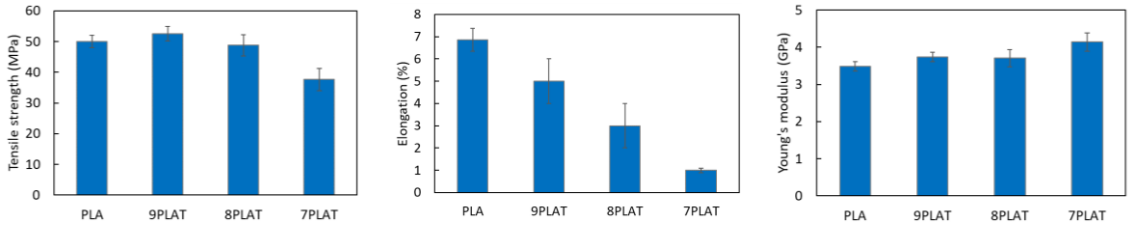


Figure 3. FTIR spectra of tannin and acetylated tannin

3.2. Mechanical properties of PLA/AT composites

The mechanical properties of PLA and PLA/AT composites are given in Figure 4. Tensile strength of composite materials generally relies on the stress transfer capacity between fillers and polymer matrix, which is significantly affected by the interfacial adhesion of particle and matrix, particle size, as well as particle distribution (Fu et al., 2008). The dispersion of AT into a thermoplastic polymer without severe agglomeration has been previously achieved by enhancement of the hydrophobic character of tannin (Gaugler et al., 2007; Grigsby et al., 2013). Therefore, unlike native tannin-filled PLA (Anwer et al., 2015), PLA incorporated with 10% and 20% AT did not exhibit significant effects on tensile strength of the resulting composites (Figure 4, a).While PLA incorporated with 30% AT encountered a decrease of tensile strength because higher biopolymer content generally caused filler agglomeration during melt blending process could result in poor particle distribution. Besides, higher loading of AT increases its interfacial area with PLA, which worsens the situation especially in absence of interfacial adhesion due to lack of virtual chemical bonds between AT and PLA. A lower elongation at break was noticed for PLA/AT composites compared with the neat PLA (Figure 4, b), which again highlights the fact that the acetyl part as a modifying agent for tannin does not possess any plasticizing effect to balance the developed interfacial adhesion as a result of acetylation, which causes premature failure. In Figure 4 (c), Young's moduli increased as a function of AT loading since the filling component restricts the molecular mobility of the polymeric chain yielding a better static adhesion (Wacker et al., 1998). A similar result was previously noted for lignin-filled PLA system (Spiridon et al., 2015; Vila et al., 2016).



(a) (b) (c)

Figure 4. Tensile parameters of PLA/AT composites: tensile strength (a), elongation (b) and Young's modulus (c)

3.3. Differential scanning calorimeter

DSC was performed in order to detect the glass transition, crystallization and melting temperatures of PLA and PLA/AT composites. DSC thermograms of PLA and PLA incorporated with various contents of AT are shown in Figure 5 and the results from the second heating and first cooling cycles are collected in Table 2. The incorporation of AT showed no significant effect on the melting (T_m) and the glass transition (T_g) temperatures, are consistent with prior studies (Anwer et al., 2015; Grigsby et al., 2014; Grigsby and Kadla, 2014). This means AT has little influence on intermolecular interactions or chain flexibility of PLA polymer chains (Müller et al., 2014). While the enhancement of T_c refers to the composite filaments are more difficult to undergo cold crystallization in comparison with pure PLA filaments and so require higher temperatures (Dong et al., 2017). As can be found in Table 2, the crystallinity of PLA/AT composites` is gradually decreasing with a corresponding decrease in the enthalpy of crystallization as a function of AT content. Therefore, the PLA/AT composites became too amorphous to be more liable to undergo higher degradation rates. This feature most likely benefits to the short-term application like implantable devices in biomedical applications (Lyu and Untereker, 2009) since the degradation of PLA occurs during a generally long period (Karamanlioglu et al., 2017; Tokiwa and Calabia, 2006).

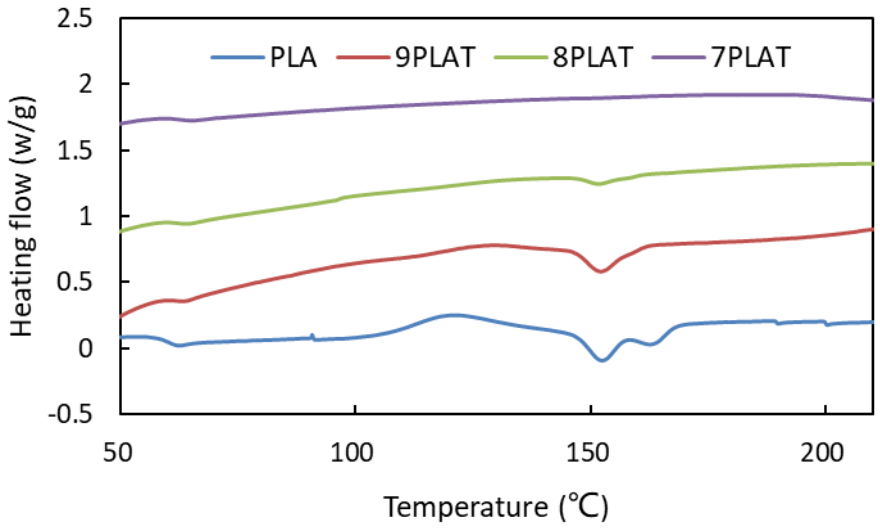


Figure 5.DSC thermograms of PLA and PLA/AT composites

Table 2. DSC results of PLA and PLA/AT composites

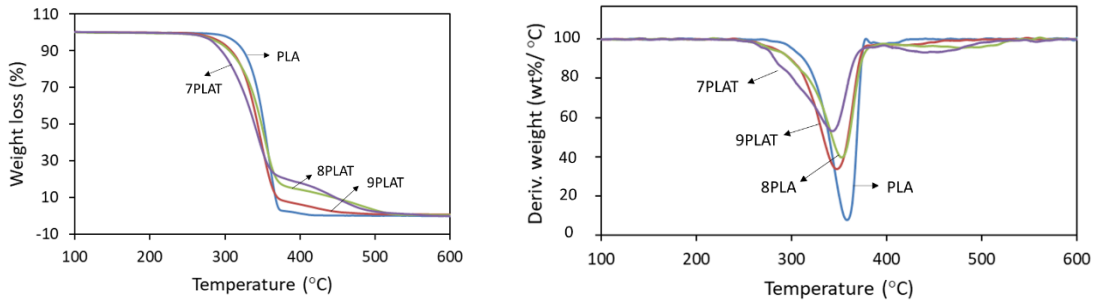
Sample	T_g (°C)	ΔH_c (J/g)	T_c (°C)	ΔH_m (J/g)	T_m (°C)	X_c (%)
PLA	56.7	14.2	120.2	20.4	152.5	6.6
9PLAT	56.3	4.23	127.5	10.9	152.6	7.9
8PLAT	56.8	0.78	129.4	3.01	151.9	3.0
7PLAT	58.6	0.26	129.7	0.06	151.1	--

Note: "--" means that no crystallization percentage.

3.4. Thermogravimetric analysis

The thermal behavior of PLA and PLA/AT composites was studied via thermogravimetric analysis under air atmosphere. The weight loss and DTG data are plotted in Figure 6as a function of temperature. Each sample sharply degraded in a one-step process started at 250°C and continued to 370°C, which is also corroborated from the single peak in the DTG profile. The results demonstrated additionally that the incorporation of AT into to PLA matrix resulted in a decrease of the thermal stability, presumably due to the drop in crystallinity (see Table 2). This observation is generally found in PLA biocomposites (Boruvka et al., 2019; Grigsby et al., 2014; Zhang et al.,

2017). The onset of degradation for all PLA/AT composites was very close to pristine PLA (250°C) while the major decomposition took place at 350°C. Consequently, a printing temperature below 250°C is considered suitable for PLA/AT composites and no decomposition should be undertaken under these conditions.



(a) (b)

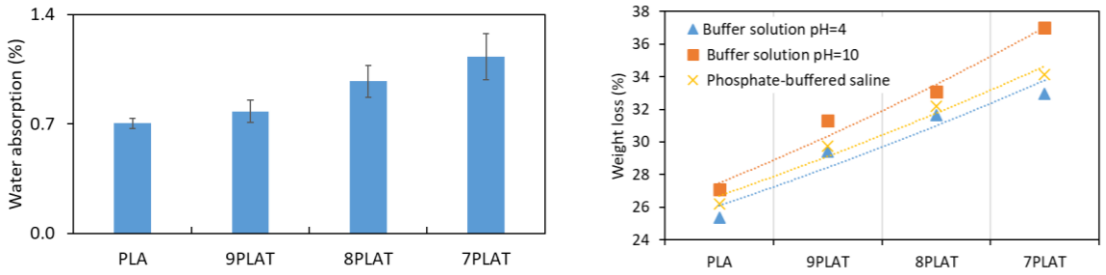
*Figure 6. Thermal gravimetric traces of PLA and PLA/AT composites (**a**) and their relevant DTG curves (**b**).*

3.5. Water absorption and degradation in solvent

PLA is a well-known degradable polymer, however, the total degradation of PLA into carbon dioxide, water, and methane in the environment generally lasts from several months to two years (Karamanlioglu et al., 2017). Moisture easily results in the hydrolyzation of PLA, therefore, water absorption capacity has been considered as an important factor to the degradability of PLA (Yew et al., 2005) when exposed to humid atmosphere. Degradation behavior of material in different pH condition is an important characteristic for many applications.

As presented in Figure 7 (a), PLA/AT composites exhibited a higher water absorption compared with the neat PLA, which may result from the decrease of crystallinity. The water absorption is related to its rate of diffusion into the composites and responsible for faster degradation of PLA/AT composites in various aqueous solutions (Figure 7, b). This characteristic is positive for medical applications because the PLA-based implants are firstly hydrolyzed in vivo by body fluids after absorbing water, which causes the breaking of the ester bonds (Yew et al., 2005). In this study, the phosphate-buffered saline (PBS) solution (pH=7.4) was used to represent the body fluids in neutral

conditions, while phosphate buffer (pH=4.0) and sodium carbonate buffer (pH=10) are applied to investigate the degradation of composite material in acidic and basic conditions. All tested samples in aqueous environments exhibited higher degradation rate with increasing the AT content. The faster degradation that appeared in strongly basic condition is the easier random ester cleavage, whereas, under acidic conditions, it proceeds via chain-end cleavage, which is more time-consuming (Elsawy et al., 2017).



(a) (b)

Figure 7. Water absorption of PLA with various AT contents over 30 days(a) and degradation in different solvent media over 50 days (b).

3.6. PLA/AT composites for 3D printing application

Color is an important appearance factor for 3D printing products. As can be seen from Table 3, PLA is a colorless transmitting polymer. The combination of PLA with dyes for producing vibrant colors is necessary for commercial applications (Scheyer and Chiweshe, 2001). From the optical image of the filaments (Table 3), PLA/ATcomposites displayed brown colors and lost transmitting characteristic. These composites had lower L* value which translates into a decrease of lightness. When PLA was compounded with more AT, an increasing trend was observed from the increasing a*and b* values, exhibiting more green hue and blue hue, respectively. Therefore, PLA/AT composites could be promising colored filaments for 3D printing products.

Table 3. Color measurements of PLA and PLA/AT composite

sample	Image of PLA and PLA/AT composites	L*	a*	b*

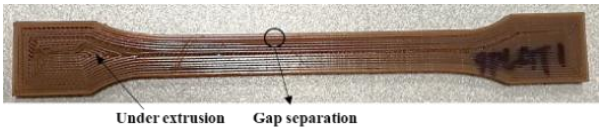
PLA		70.93	+0.91	+5.43
9PLAT		28.07	+7.91	+7.80
8PLAT		29.77	+9.09	+10.05
7PLAT		31.42	+10.22	+8.41

The model of dog bone specimens for tensile testing was used to evaluate the printability of PLA/AT composites, the printed specimens and their tensile strength results are collected in Table 4. The digital images of printed PLA/AT composites

revealed that the specimens exhibited some defects during printing, either under-extrusions or in fill and outline separations. These printed issues are not only due to the setting of the printing parameter but also may be caused by the imperfect dispersion and agglomeration of the filler (Filgueira et al., 2017). Imperfect printing is commonly found in composite materials given that the presence of fillers in polymeric matrixes change their characteristics and consequently affect their printability (Nguyen et al., 2018). Therefore, a correlation between the features of printing process with the AT-filled composite filaments is a key factor to obtain qualified printed objects. This issue will be considered more intensively in our future work.

The materials derived from the melt-extrusion 3D printing process commonly showed a lower tensile strength compared to comparable specimens obtained by traditional manufacturing methods (Cruz Sanchez et al., 2017). The relatively higher porosity of the dog bones caused during 3D printing may probably justify this finding (Filgueira et al., 2017). Another possible reason could be related to the poor interlayer adhesion of the printed specimens because the mechanical properties of printed part depends on the interlayer adhesion (Bakrani Balani et al., 2019). As a whole, the strength of printed specimen was very close to that processed by traditional manufacturing methods (Figure 4).

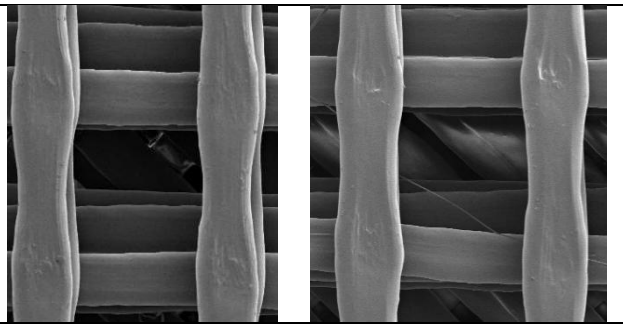
Table 4. Printed dog bone specimens and their tensile parameters

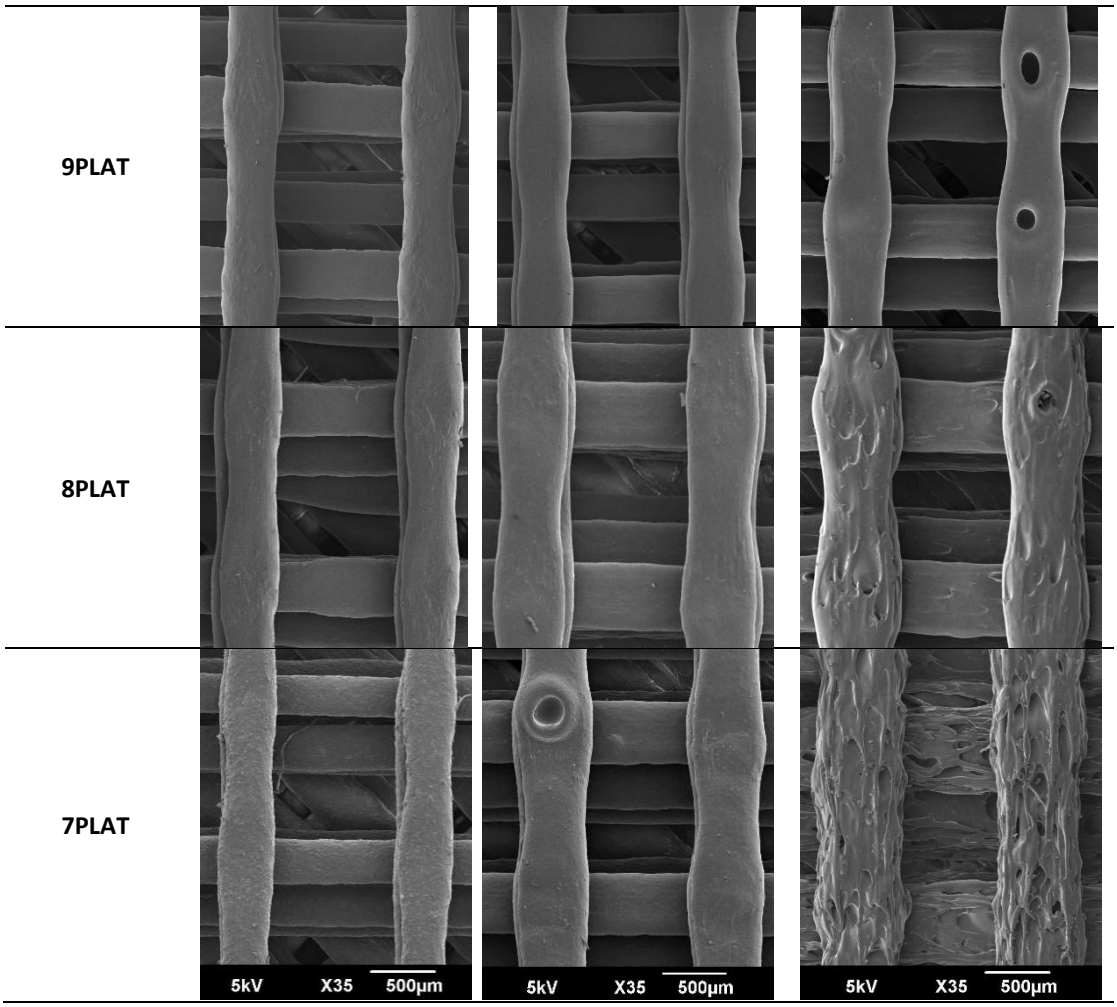
specimen	Image	Young's modulus GPa	Tensile strength MPa
PLA		2.6	27
9PLAT		2.1	26
7PLAT		2.9	31

For a specific material, the temperature is one of the most important parameters to control the shear viscosity and flow rate for offering successive layer deposition. The dimensional stability of each printed layer depends on the rapid solidification capacity via improved heat dissipation (Nguyen et al., 2018). Thus, the temperature should be carefully selected for validating the balance between flowability and solidification. For this purpose, the effects of temperature on the printability of PLA/AT composites and morphology of printed specimens were investigated by printing a scaffold prototype.

SEM images of the printed scaffolds at different temperatures are displayed in Table 5. Filaments made from PLA/AT composites are printable at a temperature range from 180 to 220°C. However, the surface morphology was mostly affected especially at higher temperatures. It is worth to notice that both lower and higher printing temperatures result in unsatisfying faults on the surface, namely, high roughness and phase separation, respectively, when PLA incorporated with a higher AT content (e.g. 7PLAT). This highlights a strong correlation between high AT loading in the filaments and the sensitivity to encounter phase separation at high temperatures. Similar results were found for a system based on hemicellulose-filled filaments (Xu et al., 2018). The unsuccessful printing of PLA scaffold at 180°C is referred to the failure of the first layer that should be stuck to the building platform. This might due to the fast cooling of extruded PLA before bonding to the building platform or to the poor flowability of PLA at 180°C. In other words, the addition of AT reduced the melting viscosity of PLA polymer (rheology behavior data in supplementary material, Figure S1), thus improved the printability even at low temperature.

Table 5. SEM images of printed scaffolds at different 3D printing temperatures

Temperature	**180°C**	**200°C**	**220°C**
PLA	Failed to print the scaffold.		



4. Conclusions

This study investigated the properties and 3D printability of a composite made from PLA and acetylated tannin. The acetylation of tannin contributed to its well dispersion within PLA matrix, guaranteeing successful fabrication of PLA/AT composite filaments via a twin-screw extruder. PLA incorporated with 20 wt% acetylated tannin did not significantly encounter deterioration in tensile property of the final product. Meanwhile, the incorporation of various AT contents caused no significant effect on the melting and glass transition temperatures of PLA because it has little influence on intermolecular interactions or chain flexibility of PLA polymer chain. A decrease of crystallinity was found in PLA/AT composites, resulting in higher rates of degradation in aquatic system especially under alkaline conditions, which would definitely benefit in short-term applications like implantable devices in biomedical field. A 3D printing temperature

below 250°C is suggested for safe processing of PLA/AT composites without encountering decomposition according to the data of thermogravimetric analysis. Although PLA systems loaded with acetylated tannin showed good printability in general, this is limited to temperatures reasonably below 220°C to avoid printing defects caused by phase separation and aggregation of acetylated tannin, especially at high loading content.

Author contributions

The manuscript was written through contributions of all authors. All authors have given approval to the final version of the manuscript.

Conflict of interest

The authors declared that they have no conflicts of interest.

Acknowledgement

This work was supported by the National Natural Science Foundation of China (NSFC 31760187, 31971595); Natural Science Foundation of Yunnan (2017FB060); and the Yunnan provincial youth and middle-age reserve talents of academic and technical leaders (2019HB026). LERMAB is supported by the French National Research Agency through the Laboratory of Excellence ARBRE (ANR-12-LABXARBRE-01). Pascal Xanthopoulos and Polybridge® are thanked for the fruitful discussions. Financial support from China Scholarship Council is gratefully acknowledged. The authors also thank Richard Laine for precious technical support.

5. References

Ambrogi, V., Cerruti, P., Carfagna, C., Malinconico, M., Marturano, V., Perrotti, M., Persico, P., 2011. Natural antioxidants for polypropylene stabilization. Polym. Degrad. Stab. 96, 2152–2158. https://doi.org/10.1016/j.polymdegradstab.2011.09.015

Anwer, M., Naguib, H.E., Celzard, A., Fierro, V., 2015. Comparison of the thermal, dynamic mechanical and morphological properties of PLA-Lignin & PLA-Tannin particulate green composites. Compos Part B Eng 82, 92–99. https://doi.org/10.1016/j.compositesb.2015.08.028

Bajpai, P.K., Singh, I., Madaan, J., 2014. Development and characterization of PLA-based green composites: A review. J. Thermoplast. Compos. Mater. 27, 52–81. https://doi.org/10.1177/0892705712439571

Bakrani Balani, S., Chabert, F., Nassiet, V., Cantarel, A., 2019. Influence of printing parameters on the stability of deposited beads in fused filament fabrication of poly(lactic) acid. Addit. Manuf. 25, 112–121. https://doi.org/10.1016/j.addma.2018.10.012

Basu, A., Nazarkovsky, M., Ghadi, R., Khan, W., Domb, A.J., 2017. Poly(lactic acid)- based nanocomposites. Polym. Adv. Technol. 28, 919–930. https://doi.org/10.1002/pat.3985

Boruvka, M., Behalek, L., Lenfeld, P., Ngaowthong, C., Pechociakova, M., 2019. Structure-related properties of bionanocomposites based on poly(lactic acid), cellulose nanocrystals and organic impact modifier. Mater. Technol. 34, 143–156. https://doi.org/10.1080/10667857.2018.1540332

Bridson, J., Kaur, J., Zhang, Z., Donaldson, L., Fernyhough, A., 2015. Polymeric flavonoids processed with co-polymers as UV and thermal stabilisers for polyethylene films. Polym Degrad Stabil 122, 18–24. https://doi.org/10.1016/j.polymdegradstab.2015.10.002

Cruz Sanchez, F.A., Boudaoud, H., Hoppe, S., Camargo, M., 2017. Polymer recycling in an open-source additive manufacturing context: Mechanical issues. Addit. Manuf. 17, 87–105. https://doi.org/10.1016/j.addma.2017.05.013

Dong, J., Li, M., Zhou, L., Lee, S., Mei, C., Xu, X., Wu, Q., 2017. The influence of grafted cellulose nanofibers and postextrusion annealing treatment on selected properties of poly(lactic acid) filaments for 3D printing. J. Polym. Sci. Part B Polym. Phys. 55, 847–855. https://doi.org/10.1002/polb.24333

Elsawy, M.A., Kim, K.-H., Park, J.-W., Deep, A., 2017. Hydrolytic degradation of polylactic acid (PLA) and its composites. Renew. Sustain. Energy Rev. 79, 1346–1352. https://doi.org/10.1016/j.rser.2017.05.143

Filgueira, D., Holmen, S., Melbø, J.K., Moldes, D., Echtermeyer, A.T., Chinga-Carrasco, G., 2017. Enzymatic-Assisted Modification of Thermomechanical Pulp Fibers To Improve the Interfacial Adhesion with Poly(lactic acid) for 3D Printing. ACS Sustain. Chem. Eng. 5, 9338–9346. https://doi.org/10.1021/acssuschemeng.7b02351

Fu, S.-Y., Feng, X.-Q., Lauke, B., Mai, Y.-W., 2008. Effects of particle size, particle/matrix interface adhesion and particle loading on mechanical properties of particulate–polymer composites. Compos. Part B Eng. 39, 933–961. https://doi.org/10.1016/j.compositesb.2008.01.002

García, D., Glasser, W., Pizzi, A., Paczkowski, S., Laborie, M.-P., 2015. Modification of condensed tannins: from polyphenol chemistry to materials engineering. New J Chem 40, 36–49. https://doi.org/10.1039/C5NJ02131F

García, D.E., Glasser, W.G., Pizzi, A., Paczkowski, S., Laborie, M.-P., 2015. Hydroxypropyl tannin from Pinus pinaster bark as polyol source in urethane

chemistry. Eur. Polym. J. 67, 152–165. https://doi.org/10.1016/j.eurpolymj.2015.03.039
Gaugler, M., Grigsby, W., Harper, D., Rials, T., 2007. Chemical imaging of the spatial distribution and interactions of tannin dispersal in bioplastic systems. Adv. Mater. Res. 29–30, 173–176. https://doi.org/10.4028/www.scientific.net/AMR.29-30.173
Ge, J., Shi, X., Cai, M., Wu, R., Wang, M., 2003. A novel biodegradable antimicrobial PU foam from wattle tannin. J. Appl. Polym. Sci. 90, 2756–2763. https://doi.org/10.1002/app.12928
Gkartzou, E., Koumoulos, E.P., Charitidis, C.A., 2017. Production and 3D printing processing of bio-based thermoplastic filament. Manuf. Rev. 4, 1. https://doi.org/10.1051/mfreview/2016020
Grigsby, W., Bridson, J., Lomas, C., Frey, H., 2014. Evaluating Modified Tannin Esters as Functional Additives in Polypropylene and Biodegradable Aliphatic Polyester. Macromol Mater Eng 299, 1251–1258. https://doi.org/10.1002/mame.201400051
Grigsby, W., Kadla, J., 2014. Evaluating Poly(lactic acid) Fiber Reinforcement with Modified Tannins. Macromol Mater Eng 299, 368–378. https://doi.org/10.1002/mame.201300174
Grigsby, W.J., Bridson, J.H., Lomas, C., Elliot, J.-A., 2013. Esterification of Condensed Tannins and Their Impact on the Properties of Poly(Lactic Acid). Polymers 5, 344–360. https://doi.org/10.3390/polym5020344
Grigsby, W.J., Bridson, J.H., Schrade, C., 2015. Modifying biodegradable plastics with additives based on condensed tannin esters. J Appl Polym Sci 132, 41626. https://doi.org/10.1002/app.41626
Guo, R., Ren, Z., Bi, H., Song, Y., Xu, M., 2018. Effect of toughening agents on the properties of poplar wood flour/poly (lactic acid) composites fabricated with Fused Deposition Modeling. Eur. Polym. J. 107, 34–45. https://doi.org/10.1016/j.eurpolymj.2018.07.035
Hussain, T., Tausif, M., Ashraf, M., 2015. A review of progress in the dyeing of eco-friendly aliphatic polyester-based polylactic acid fabrics. J. Clean. Prod. 108, 476–483. https://doi.org/10.1016/j.jclepro.2015.05.126
Kai, D., Tan, M.J., Chee, P.L., Chua, Y.K., Yap, Y.L., Loh, X.J., 2016. Towards lignin-based functional materials in a sustainable world. Green Chem. 18, 1175–1200. https://doi.org/10.1039/C5GC02616D
Karamanlioglu, M., Preziosi, R., Robson, G.D., 2017. Abiotic and biotic environmental degradation of the bioplastic polymer poly(lactic acid): A review. Polym. Degrad. Stab. 137, 122–130. https://doi.org/10.1016/j.polymdegradstab.2017.01.009
Koleckar, V., Kubikova, K., Rehakova, Z., Kuca, K., Jun, D., Jahodar, L., Opletal, L., 2008. Condensed and hydrolysable tannins as antioxidants influencing the health. Mini Rev. Med. Chem. 8, 436–447. https://doi.org/10.2174/138955708784223486
Lai So, V.L., He, L., Xin, J.H., 2014. Bio-inspired colouration on various textile materials using a novel catechol colorant. RSC Adv 4, 41081–41086. https://doi.org/10.1039/C4RA06004K
Lee, J.-Y., An, J., Chua, C.K., 2017. Fundamentals and applications of 3D printing for novel materials. Appl. Mater. Today 7, 120–133. https://doi.org/10.1016/j.apmt.2017.02.004
LI, T., Aspler, J., Kingsland, A., 2016. 3D PRINTING – A REVIEW OF

TECHNOLOGIES, MARKETS, AND OPPORTUNITIES FOR THE FOREST INDUSTRY. Can. Makes. URL http://canadamakes.ca/3d-printing-review-technologies-markets-opportunities-forest-industry/ (accessed 12.4.19).
Liao, J., Brosse, N., Pizzi, A., Hoppe, S., 2019. Dynamically Cross-Linked Tannin as a Reinforcement of Polypropylene and UV Protection Properties. Polymers 11, 102. https://doi.org/10.3390/polym11010102
Liu, J., Sun, L., Xu, W., Wang, Q., Yu, S., Sun, J., 2019. Current advances and future perspectives of 3D printing natural-derived biopolymers. Carbohydr. Polym. 207, 297–316. https://doi.org/10.1016/j.carbpol.2018.11.077
Long, H., Wu, Z., Dong, Q., Shen, Y., Zhou, W., Luo, Y., Zhang, C., Dong, X., 2019. Mechanical and thermal properties of bamboo fiber reinforced polypropylene/polylactic acid composites for 3D printing. Polym. Eng. Sci. 59, E247–E260. https://doi.org/10.1002/pen.25043
Luo, C., Grigsby, W., Edmonds, N., Easteal, A., Al-Hakkak, J., 2010. Synthesis, characterization, and thermal behaviors of tannin stearates prepared from quebracho and pine bark extracts. J. Appl. Polym. Sci. 17, 352–360. https://doi.org/10.1002/app.31545
Lyu, S., Untereker, D., 2009. Degradability of Polymers for Implantable Biomedical Devices. Int. J. Mol. Sci. 10, 4033–4065. https://doi.org/10.3390/ijms10094033
Müller, A.J., Ávila, M., Saenz, G., Salazar, J., 2014. CHAPTER 3. Crystallization of PLA-based Materials, in: Jiménez, A., Peltzer, M., Ruseckaite, R. (Eds.), Polymer Chemistry Series. Royal Society of Chemistry, Cambridge, pp. 66–98. https://doi.org/10.1039/9781782624806-00066
Murariu, M., Dubois, P., 2016. PLA composites: From production to properties. Adv. Drug Deliv. Rev., PLA biodegradable polymers 107, 17–46. https://doi.org/10.1016/j.addr.2016.04.003
Nguyen, N.A., Barnes, S.H., Bowland, C.C., Meek, K.M., Littrell, K.C., Keum, J.K., Naskar, A.K., 2018. A path for lignin valorization via additive manufacturing of high-performance sustainable composites with enhanced 3D printability. Sci. Adv. 4, eaat4967. https://doi.org/10.1126/sciadv.aat4967
Nicollin, A., Zhou, X., Pizzi, A., Grigsby, W., Rode, K., Delmotte, L., 2013. MALDI-TOF and 13C NMR analysis of a renewable resource additive—Thermoplastic acetylated tannins. Ind. Crops Prod. 49, 851–857. https://doi.org/10.1016/j.indcrop.2013.06.013
Olejar, K.J., Ray, S., Kilmartin, P.A., 2016. Enhanced antioxidant activity of polyolefin films integrated with grape tannins: Enhanced antioxidant activity of polyolefin films integrated with grape tannins. J. Sci. Food Agric. 96, 2825–2831. https://doi.org/10.1002/jsfa.7450
Pizzi, A., 1980. Tannin-Based Adhesives. J. Macromol. Sci. Part C 18, 247–315. https://doi.org/10.1080/00222358008081043
Ren, J., 2011. Biodegradable poly (lactic acid) synthesis, modification, processing and applications. Tsinghua University Press : Springer, Beijing; Heidelberg.
Samper, M.D., Fages, E., Fenollar, O., Boronat, T., Balart, R., 2013. The potential of flavonoids as natural antioxidants and UV light stabilizers for polypropylene. J. Appl. Polym. Sci. 129, 1707–1716. https://doi.org/10.1002/app.38871
Scheyer, L.E., Chiweshe, A., 2001. Application and Performance of Disperse Dyes on

Polylactic Acid (PLA) Fabric. AATCC Mag. 1, 44–48.
Shnawa, H., Khaleel, M., Muhamed, F., 2015. Oxidation of HDPE in the Presence of PVC Grafted with Natural Polyphenols (Tannins) as Antioxidant. J. Polym. Chem. 05, 9–16. https://doi.org/10.4236/ojpchem.2015.52002
Smith, B.C., 2018. The C=O Bond, Part IV: Acid Anhydrides [WWW Document]. URL http://www.spectroscopyonline.com/co-bond-part-iv-acid-anhydrides (accessed 4.16.19).
Tappa, K., Jammalamadaka, U., 2018. Novel Biomaterials Used in Medical 3D Printing Techniques. J. Funct. Biomater. 9. https://doi.org/10.3390/jfb9010017
Tokiwa, Y., Calabia, B.P., 2006. Biodegradability and biodegradation of poly(lactide). Appl. Microbiol. Biotechnol. 72, 244–251. https://doi.org/10.1007/s00253-006-0488-1
Tomak, E.D., Arican, F., Gonultas, O., Sam, E.D., 2018. Influence of tannin containing coatings on weathering resistance of wood: Water based transparent and opaque coatings. https://doi.org/10.1016/j.polymdegradstab.2018.03.011
Vila, C., Santos, V., Saake, B., Parajó, J.C., 2016. Manufacture, Characterization, and Properties of Poly-(lactic acid) and its Blends with Esterified Pine Lignin. BioResources 11, 5322–5332. https://doi.org/10.15376/biores.11.2.5322-5332
Xu, W., Pranovich, A., Uppstu, P., Wang, X., Kronlund, D., Hemming, J., Öblom, H., Moritz, N., Preis, M., Sandler, N., Willför, S., Xu, C., 2018. Novel biorenewable composite of wood polysaccharide and polylactic acid for three dimensional printing. Carbohydr. Polym. 187, 51–58. https://doi.org/10.1016/j.carbpol.2018.01.069
Yamoum, C., Maia, J., Magaraphan, R., 2017. Rheological and thermal behavior of PLA modified by chemical crosslinking in the presence of ethoxylated bisphenol A dimethacrylates 28, 102–112. https://doi.org/10.1002/pat.3864
Yew, G.H., Mohd Yusof, A.M., Mohd Ishak, Z.A., Ishiaku, U.S., 2005. Water absorption and enzymatic degradation of poly(lactic acid)/rice starch composites. Polym. Degrad. Stab. 90, 488–500. https://doi.org/10.1016/j.polymdegradstab.2005.04.006
Zhai, Y., Wang, J., Wang, H., Song, T., Hu, W., Li, S., 2018. Preparation and Characterization of Antioxidative and UV-Protective Larch Bark Tannin/PVA Composite Membranes. Molecules 23, 2073. https://doi.org/10.3390/molecules23082073
Zhang, L., Lv, S., Sun, C., Wan, L., Tan, H., Zhang, Y., 2017. Effect of MAH-g-PLA on the Properties of Wood Fiber/Polylactic Acid Composites. Polymers 9, 591. https://doi.org/10.3390/polym9110591